Functional Coating: Effect of Particle Morphology on Photocatalytic Activity of Titanium Dioxide Nanoparticles

Naphat Thiwakornkitkul

A Report Submitted in Partial Fulfillment of the Requirements
for the Degree of Bachelor of Engineering (Petrochemical Engineering)
Department of Chemical Engineering, Faculty of Engineering,
King Mongkut's Institute of Technology Ladkrabang
Academic Year 2016

ชั้นเคลือบผิวพิเศษ: ผลของโครงสร้างสัณฐานของอนุภาคไทเทเนียมไดออกไซด์ต่อสมบัติการเร่งปฏิกิริยาด้วยแสง

นภัทร ทิวากรกิจกุล

ปริญญานิพนธ์นี้เป็นส่วนหนึ่งของการศึกษาตามหลักสูตร
วิศวกรรมศาสตรบัณฑิต สาขาวิชาวิศวกรรมปิโตรเคมี
ภาควิชาวิศวกรรมเคมี คณะวิศวกรรมศาสตร์
สถาบันเทคโนโลยีพระจอมเกล้าเจ้าคุณทหารลาดกระบัง
ปีการศึกษา 2559

Title	Functional Coating: Effect of Particle Morphology on Photocatalytic Activity of Titanium Dioxide Nanoparticles
By	Naphat Thiwakornkitkul ID. 56010645
Field of Study	Petrochemical Engineering
Advisor	Asst. Prof. Dr. Teerapon Suteewong

Accepted by the Faculty of Engineering, King Mongkut's Institute of Technology Ladkrabang in Partial Fulfillment of the Requirements for the Degree of Bachelor of Engineering (Petrochemical Engineering).

Thesis Committee

T. Suteewong
(Asst. Prof. Dr. Teeraporn Suteewong) Chairman

(Assoc. Prof. Dr. Duangkamol Na-Ranong) Committee

Apinan Namkanisorn
(Asst. Prof. Dr. Apinan Namkanisorn) Committee

Title	Functional Coating: Effect of Particle Morphology on Photocatalytic Activity of Titanium Dioxide Nanoparticles
By	Naphat Thiwakornkitkul ID. 56010645
Field of Study	Petrochemical Engineering
Advisor	Asst. Prof. Dr. Teerapon Suteewong
Affiliation	Department of Chemical Engineering, King Mongkut's Institute of Technology Ladkrabang

Abstract

Dispersing another materials in the matrix to form composite is one of general methods to render special functions to a coating layer. Titanium dioxide (TiO_2), known for its photocatalytic activity (PCA) that can be used to degrade volatile organic substances and to protect microbial infection, is considered to be an interesting dispersed-specie. However, intense light is often required to achieve high photocatalytic activity. Scattering layer composing of hollow TiO_2 nanoparticles is known as light harvester in solar cell devices which may be able to be used for photocatalysis function with lower light intensity. In this work, we have studied an effect of hollow morphology to the PCA of TiO_2 nanoparticles. Hollow TiO_2 nanoparticles were successfully synthesized using hard-template-assisted sol-gel method. Transmission electron microscope (TEM) images show that synthesized hollow TiO_2 have 125 nm hollow core diameter and 50 nm thick TiO_2 shell thickness. For Dense TiO_2, particle size was around 150 nm. Particle size distribution is relatively narrow. XRD results revealed no peak for calcined and non-calcined samples, on the other hand, difference for each sample was reported by UV-DRS results. Comparison between hollow and dense TiO_2, UV-DRS spectrum showed the higher diffuse reflectance for both hollow TiO_2 samples, proven for multiple light scattering and reflection to be occurred. However, they came with higher energy bandgap of 3.76 eV for amorphous and 3.58 eV for calcined samples. For dense TiO_2, 3.53 and 3.36 eV were the bandgaps of amorphous and calcined samples, respectively.

Keywords: TiO_2, Hollow nanoparticles, Coating, Photocatalysis

เรื่อง	ชั้นเคลือบผิวพิเศษ: ผลของโครงสร้างสัณฐานของอนุภาคไทเทเนียมไดออกไซด์ต่อสมบัติการเร่งปฏิกิริยาด้วยแสง
โดย	นภัทร ทิวากรกิจกุล รหัส **56010645**
สาขาวิชา	วิศวกรรมปิโตรเคมี
อาจารย์ที่ปรึกษา	ผศ.ดร. ธีรพร สุธีวงศ์
สังกัด	ภาควิศวกรรมเคมี สถาบันเทคโนโลยีพระจอมเกล้าเจ้าคุณทหารลาดกระบัง

บทคัดย่อ

การนำวัสดุต่างชนิด มาผสมในชั้นแมทริกซ์เป็นชั้นเคลือบคอมพอสิตนับเป็นอีกหนึ่งวิธีที่นิยมใช้สำหรับการสร้างชั้นเคลือบผิวที่มีคุณสมบัติพิเศษ อนุภาคไทเทเนียมไดออกไซด์นั้นเป็นวัสดุที่น่าสนใจสำหรับการนำมาทำชั้นเคลือบคอมพอสิต เนื่องจากมีสมบัติในการเร่งปฏิกิริยาด้วยแสงที่สามารถนำไปใช้ย่อยสลายสารระเหยอินทรีย์และยับยั้งเชื้อจุลินทรีย์ได้ อย่างไรก็ตามการเร่งปฏิกิริยาดังกล่าวมักต้องการแสงที่มีความเข้มข้นสูงเพื่อให้ผลมีประสิทธิภาพ เป็นที่รู้กันดีว่าไทเทเนียมไดออกไซด์รูปทรงกลวงได้ถูกใช้เพื่อเพิ่มความสามารถในการรับแสงของโซลาร์เซลล์ ซึ่งอาจนำมาประยุกต์ใช้ในการเร่งปฏิกิริยาโดยอาศัยแสงน้อยลงได้ จึงเป็นที่มาของปริญญานิพนธ์นี้คือการศึกษาผลของโครงสร้างอนุภาคทรงกลวงต่อการเร่งปฏิกิริยาด้วยแสง การทดลองนี้ทำการเตรียมอนุภาคนาโนไทเทเนียมไดออกไซด์รูปทรงกลวงด้วยวิธีโซลเจลโดยใช้แม่แบบชนิดแข็งเป็นแม่พิมพ์แล้วหุ้มด้วยชั้นไททาเทียมไดออกไซด์ จากการตรวจสอบขนาดและโครงสร้างสัณฐานของอนุภาคที่เตรียมได้ด้วยกล้องจุลทรรศน์อิเล็กตรอนชนิดส่องผ่านพบว่าขนาดอนุภาคมีช่วงการกระจายที่แคบ โดยที่ส่วนกลวงของอนุภาคมีขนาดเส้นผ่านศูนย์กลาง 125 นาโนเมตร และชั้นของไทเทเนียมไดออกไซด์ที่ล้อมรอบหนา 50 นาโนเมตร ส่วนอนุภาคทรงกลมตันมีเส้นผ่านศูนย์กลางประมาณ 150 นาโนเมตร ผลการทดสอบทดสอบการเลี้ยวเบนของรังสีเอ็กซ์ชี้ให้เห็นว่าทุกตัวอย่างอยู่ในโครงสร้างอสัณฐาน อย่างไรก็ตาม ผลของเครื่อง UV-DRS ยังคงแสดงให้เห็นความแตกต่างสำหรับตัวอย่างที่ถูกเผาและไม่ถูกเผา นอกจากนี้ยังชี้ให้เห็นว่าอนุภาคไททาเนียมไดออกไซด์รูปทรงกลวงมีการสะท้อนแสงแบบกระเจิงมากกว่าทรงกลมตัน ในทางตรงกันข้าม ค่าช่องว่างระหว่างแถบพลังงาน (bandgap) ของอนุภาคไททาเนียมไดออกไซด์ที่มีรูปทรงกลวงมีค่าพลังงานอยู่ที่ 3.76 และ 3.58 eV ซึ่งสูงกว่าอนุภาครูปทรงกลมตันที่มีค่าพลังงาน 3.53 และ 3.36 eV สำหรับตัวอย่างที่ไม่ถูกเผาและถูกเผา ตามลำดับ

คำสำคัญ: ไทเทเนียมไดออกไซด์, อนุภาคนาโนรูปทรงกลวง, การเคลือบผิว, การเร่งปฏิกิริยาด้วยแสง

Acknowledgements

First of all, I would like to express my gratefulness to my thesis advisor, Asst. Prof. Dr. Teeraporn Suteewong for her helps and supports, whether in form of advised, encouragement, or positive criticizing. Not only in this project, but also in other aspects. This project report cannot be completed without these things.

Next, I appreciated every professors and staffs in the department for their comments and helps on this project which provide more eases for the researching progress.

In the end, I sincerely thank all of my parent, friends, and seniors, especially Mr. Paiboon Saejear for their opinions, recommendations and countenances, which always filled my morale and made me proceeded through any disheartening contents.

Naphat Thiwakornkitkul

Table of Contents

Table of Contents

List of Figures

List of Figures

List of Tables

CHAPTER I
INTRODUCTION

1.1 Background

Incorporating dispersed nanoparticles into the polymer matrix have been practicing for over decades to provide a coating layer with improved or with novel properties. [1] Focusing on the dispersed nanoparticles, the ones that possess multifunction are considered to be an interesting choices.

Titanium dioxide (TiO_2) is a widely-used ingredient in pigments, cosmetics, and photocatalyst industry because of its expedient advantages and characteristics such as cost-effective, non-toxicity, photoactive, chemical and thermal stability. [2] In these few decades, especially after the discovery of water splitting application of TiO_2 in 1972, extensive studies have been focused on its semiconductor-based uses, such as environmental remedy (e.g. pollutants degradation), dyes-sensitized solar cell (DSSC), hydrogen production, self-cleaning surface, gas sensing, medical devices, and antimicrobial applications. [2-5]

Most of applications rely on its photocatalytic activity (PCA) as semiconductor materials. However, its photocatalytic activity is photo-intensive so that its capability might be limited to only environment that possess high intensity of light. Hence, the improvement of light intensifying properties of TiO_2 will be necessary.

Since the functions of coating layer come from integrated-materials, its efficiency could be also enhanced through modification of TiO_2 particles. Properties of TiO_2 is size-dependent. The smaller the particle size, the higher the specific surface area (SSA), resulting in more active sites. At nanoscale, the diffusion path length of electron is short, causing low rate of charge recombination. With these features, TiO_2 nanoparticles display higher photocatalytic activity than the bulk one. Moreover, photocatalytically active surface and light absorption also reveal the strong relation with PCA. As a result, further enhancement of the catalytic performance apart from synthesizing as nanoparticles can be

manipulated by controlling crystallinity, crystal phase, and morphology as well as fabricating as composite. [7-9]

With the concept of light intensification, hollow morphology is of great interest due to its unique optical properties. Hollow cavity inside the shell can perform internal multiple light scattering and refection, which enhances light harvesting ability comparing with their dense (or solid) structure counterparts. In addition, it possesses large number of active sites due to high specific surface area and short electron diffusion pathway. High surface area to volume ratio also increases the possibility of contact between reactants and active sites. [9-13]

In the early stage, because of low densities, refractive indices and thermal expansion coefficients, hollow nanoparticles have been reported to be suitable for an applications like energy storage, antireflection and catalysis as well as catalyst support. With the merit of continuous studies, improvement of mechanical, electrical and chemical properties in hollow nanoparticles expands its applicability to many new applications (e.g. drug delivery, therapeutics, fluorescence, lithium-ion batteries and biomedical). Various materials ranging from metal, metal oxide, semiconductor as well as polymer were used in those studies, for examples, gold (Au), silver (Ag), cobalt oxide (CoO), cerium dioxide (CeO_2), silica (SiO_2), zinc oxide (ZnO), polystyrene (PS) etc. [10,11]

Similarly, hollow TiO_2 have been focused on green energy aspects (e.g. DSSCs, lithium ion storage, and hydrogen production). Only a few have been examined on the hollow morphology advantages in terms of PCA for photodegradation or antimicrobial applications. Moreover, most of the available literatures involved composite hollow particles. [12,13] Yamaguchi et al. (2016) have reported on comparative study of inactivating chemical and biological substances using hollow and solid TiO_2 nanoparticles. However, the representative of hollow morphologies in their work was actually an opened-hole, cup-liked structure. [18] More precise understanding in structural effects could allow us to improve the photocatalytic activity characteristic of TiO_2.

Herein, we study the effects of the hollow structure of TiO_2 particles on photocatalytic activity in term of bandgap energy, with respect to dense particles. Facile sol-gel approach was employed for particle syntheses with the aid of silica nanoparticle template in order to form hollow structure as it provides desirable particle size and size distribution. After the formation of TiO_2 shell, silica core was removed via chemical etching method. [15] Resulting particles were then calcined to form anatase phase. Particle size and size distribution as well as morphology were investigated using transmitting electron microscope (TEM). X-ray diffraction spectroscopy (XRD) were used for characterization of crystalline phase. Finally, UV-DRS was employed to evaluate optical properties of the samples as diffuse reflectance. The reflectance data, when transformed into absorbance spectrum, can be used to calculate the bandgap. Primary comparison of photocatalytic activity were done according to the bandgap values.

1.2 Objective

To elucidate the effect of hollow morphology on photocatalytic activity of TiO_2 nanoparticles according to the bandgap energy.

1.3 Scopes of Work

1.3.1 Syntheses of dense and hollow TiO_2 nanoparticles with well-defined particle size and size distribution as well as crystalline phase.

1.3.2 Investigate the optical properties of synthesized nanoparticles

1.3.3 Evaluate the bandgap of dense and hollow TiO_2 through UV-DRS spectra.

1.4 Expected Outputs

1.4.1 Understand the PCA-enhanced optical properties of hollow sample with respect to dense structure counterparts.

1.4.2 Obtain the hollow TiO_2 with desirable properties, which could provide opportunities for further modification for a novel applications.

CHAPTER II
LITERATURE REVIEW

2.1 Titanium Dioxide

Generally known, TiO_2 can exists in many polymorphs. Commonly studied forms are anatase, rutile, and brookite. Differences in structural arrangement for each polymorph come from the way which octahedral units are connected together. [2,3] Two, three, and four shared-edges are observed for rutile, brookite, and anatase, respectively, as shown in Figure 2.1. For all polymorphs, bond distance of Ti-O is reported to be similar while the variation is found in O-O bond distances. X-ray diffraction and Raman spectroscopy as well as high resolution transmission electron microscope analysis are available techniques for crystalline phase examining. [2] Different polymorphs exhibit distinct crystalline facet, thus providing altered environments for charge carriers when they reach TiO_2 surface. [5]

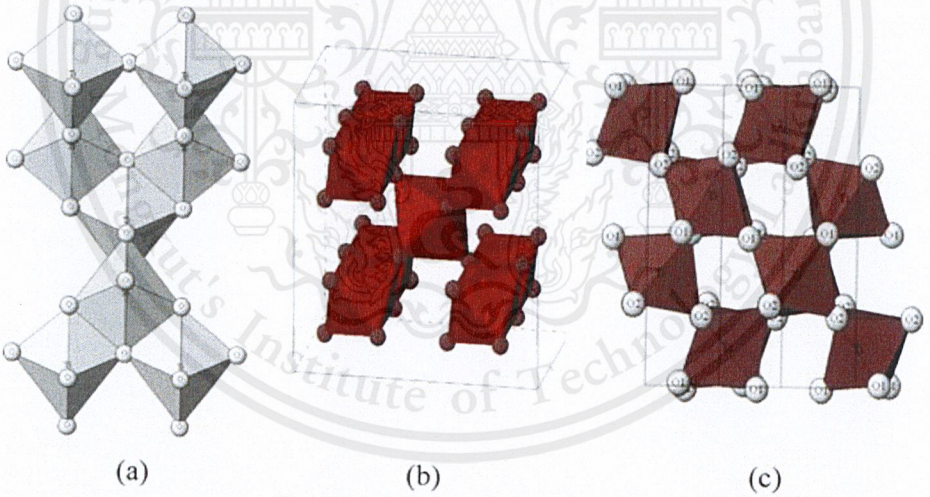

Figure 2.1. Crystalline structures of (a) anatase, (b) rutile, and (c) brookite. [3]

2.1.1 TiO_2 Photocatalysis

Fujishima et al. (2008) have written quite comprehensive review on photocatalysis and related surface phenomena of TiO_2. [5] It has been observed that when TiO_2-based paint is exposed to sunlight for a long time, the non-adhered white powder is formed, called "chalking'. This powder is produced by decomposition of organic paint components via

the photo-induced catalysis. Early studies have been focused on the chalking in TiO_2-based paint, then gradually shifted into a very interesting study topic, i.e., photocatalysis, which provides an expedient means for environmental remedies, self-cleaning surface, antimicrobial as well as energy applications. [2,3] One of the important breakthrough is the discovery of water splitting with TiO_2 in 1972. [5]

As described in the literature, photocatalysis involves the generation of electrons and holes. TiO_2 were reported to be an N-type semiconductor due to the formation of oxygen vacancies. [3] As semiconductor material, TiO_2 requires certain energy level, depending on the band gap, to activate its conductor characteristic by generating mobile electron from electron excitation. Band gap is the energy difference between valence band and conduction band which represents amount of energy level required for electron excitation. Rutile and anatase are reported to possess a band gap energy of approximately 3.0 and 3.2 eV, respectively. [3-5]

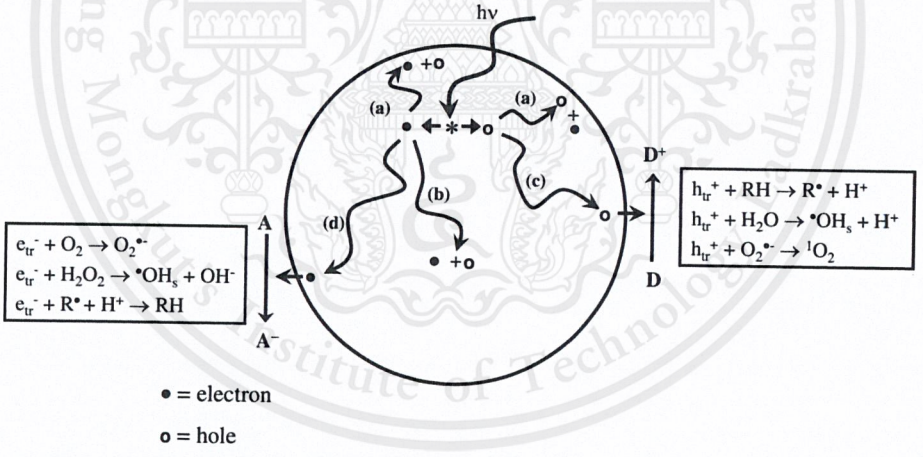

Figure 2.2. Schematic diagram represents for the phenomena occurring in bare TiO_2 after UV excitation; a) and b) Charge recombination near surface and in bulk matrix, respectively, c) oxidation and d) reduction sites (interfacial charge transfer).

In photocatalysis, when the required energy of light is irradiated on TiO_2 material, electrons are excited and leave electron holes behind, resulting in electron-hole pairs. Generated electrons can move freely throughout the matrix of photocatalysts. Meanwhile, holes is virtually moved by electron hopping from the adjacent position. Separated charge carriers (electrons and holes) will become an active sites for redox reaction when they reach

the surface. This is the key mechanism in photocatalysis. On the other hand, while charge carriers are travelling, they can recombine with each other, which then emits heat or become luminescence before reverting excited electron back to valence band state. In this scenario, photocatalysis is not observed. These phenomena are called charge generation (charge separation), interfacial charge transfer, and charge recombination, respectively (see Figure 2.2). [3-5]

Equations related in photocatalysis mechanisms can be written as follow: [5]

- Charge carriers generation:

$$TiO_2 + hv \rightarrow e^- (excited\ electron) + h^+ (electron\ hole) \quad (2.1)$$

- Charge recombination:

$$e^- + h^+ \rightarrow heat\ (or\ hv) \quad (2.2)$$

- Interfacial charge transfer:

$$h^+ + e^-\ donor \rightarrow reduced\ product \quad (2.3)$$

$$e^- + e^-\ acceptor \rightarrow oxidized\ product \quad (2.4)$$

Recall redox-reaction sites formation, electron holes, which gain electrons from the reacted substance, will act as oxidation sites resulting in either oxygen evolution, hydroxyl radical production, or oxidation of organic substances. Meanwhile, electrons which transfer from the interface between reacted substance and photocatalyst will act as reduction sites. If reacted specie is oxygen, products of the reduction reaction can be either superoxide radical, hydrogen peroxide radical, or water. On the other hand, if reacted specie is an organic substance, a reduced form of that specie is produced. Generated radicals are called "Reactive oxygen species (ROS)". [5,6] Concealed under the term "photocatalytic activity", these generated species are the one that actually act as catalyst.

Equations of these mechanism can be stated as follow: [3]

- Radical specie generation:

$$H_2O + h^+ \rightarrow \dot{O}H + H^+ (proton) \quad (2.5)$$

$$O_2 + e^- \rightarrow \dot{O_2^-} \quad (2.6)$$

$$\dot{O_2^-} + h^+ \rightarrow \dot{O}OH \quad (2.7)$$

- Hydrogen peroxide formation:

$$\dot{O}OH + \dot{O}OH \rightarrow H_2O_2 + O_2 \quad (2.8)$$

- Organic substance degradation:

$$\dot{O}H + organic\ substances \rightarrow\rightarrow\rightarrow CO_2 + H_2O \quad (2.9)$$

$$\dot{O_2^-} + organic\ substances \rightarrow\rightarrow\rightarrow CO_2 + H_2O \quad (2.10)$$

$$\dot{O}OH + organic\ substances \rightarrow\rightarrow\rightarrow CO_2 + H_2O \quad (2.11)$$

2.1.2 Photocatalytic activity improvements

Despite of difference in their objectives, one important thing that most of applications shared in common is to improve the photocatalytic activity (PCA) of TiO_2. Enhancement of the photocatalytic activity can be done by numerous ways. According to above sections, facilitating charge carrier generation and transportation as well as suppressing the charge recombination are considered as pathways to increase PCA. Much efforts were spent on these concepts in the recent decade to improve the efficacy of TiO_2 photocatalysis. [3,9,10] TiO_2 composites, as demonstrated in Dahl et al. (2014) works, have shown promising performance together with properties, opening the venue to novel applications. For example, chromium-TiO_2 composite have revealed enhanced-photocatalytic reactions as well as applicability in NO_x abatement and magnetic applications. Another material is Au-TiO_2 composite. With a tunable localized surface plasmon resonance (LSPR) and robust chemical stability, Au-TiO_2 composite is obviously promising in terms of robustness and PCA efficacy. However, involvement with toxic material, chromium, or costly, like Au, might create the limitation for study and practice. [7] Availability of TiO_2 in different morphologies is an alluring alternative route for PCA improvement. In the scope of structural design, some of TiO_2 morphologies were reviewed by Gao et al. (2015). Although they focused on core-shell and hierarchical structure, useful information was thoroughly provided. Solid sphere is referred as to zero-dimensional. Rod, wire, fiber, belt, and tube are classified as one-dimensional structures. Two-dimensional structure consist of sheet and plate. While hollow, hierarchical, and interconnected are considered as three-dimensional structures, which were fabricated by lower-dimensional

building block nanoparticles. They reported that these structures possess high surface area to volume ratio along with unique optical and charge transfer properties. Additionally, some advantageous traits of core-shell structure in term of light absorption as light scattering and up-conversion also demonstrated. [9]

2.1.3 Hollow TiO_2 structures

Hollow is considered as a derivative of core-shell structures. [9] Zhang et al. (2015) have published a review on hollow-nanostructured TiO_2 for energy and environmental applications. Besides from synthetic strategies, they also reviewed that in dye-sensitized solar cell, employment of hollow TiO_2 particles as N-type semiconductor substrate for dye-sensitizer can perform better performance of conversion efficiency compared with solid-structured counterparts. Apart from frequently-referred explanation such as higher specific surface area and larger volume (in this case, for dye storage), light scattering and reflection as well as charge collection are new additional explanations. [13] As a supplementary information, comparative study between DSSC with and without scattering layer of DSSC was examined by Dadgostar and coworkers (2012). [12] Two scattering layers were used in their study, one was constructed by TiO_2 solid particles (namely TiO_2 filled sphere: T-FS) while, in another one, TiO_2 hollow particles (T-HS) was employed. Their results proved that DSSC containing hollow TiO_2 particle as scattering layer achieved the highest energy and incident photon conversion efficiencies (IPCE) as illustrated in Figure 2.4. T-HS performance was claimed to be superior despite of lower measured scattering power when comparing with T-FS. The number of photons absorbed by T-HS is higher than that of T-FS, because hollow cavity can reflect light and extend the light path. [12]

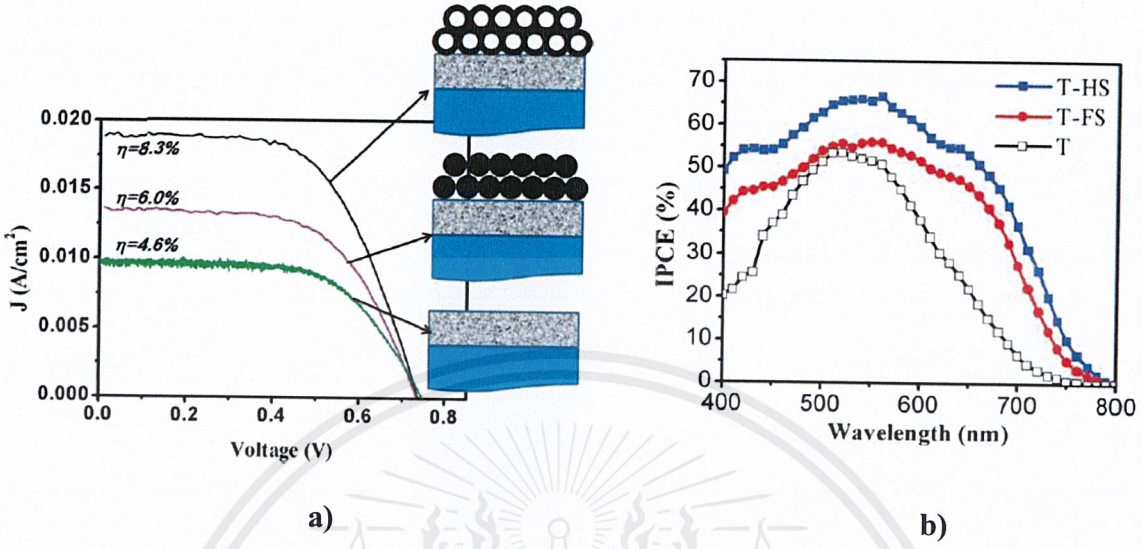

a) **b)**

Figure 2.3. a) I–V curves and b) incident photon conversion efficiency of dye-sensitized solar cell with a photoanode of a single transparent film (T) without a scattering layer, and with filled sphere (FS) and hollow sphere (HS) scattering layers.

Since the enhanced incident photon conversion efficiency in Dadgostar and coworkers study (2012) was obviously the results of increasing light harvesting ability with scattering layer, with the same concepts, photo-induced disinfection might be enhanced via similar process. [14]

Therefore, hollow TiO_2 possessing optical properties of multiple light scattering and reflection could be the answer for PCA-enhancement for the purpose to provide TiO_2 that can perform light intensification for applicability in dim environments. However, only a few number of literatures purely involved with hollow TiO_2 PCA without an integrating or other species. [12,13] Research done by Yamaguchi et al. (2016) was among those literatures, which introduced a comparative study between hollow and solid morphologies. In accordance to their results, it was concluded that performance of solid TiO_2 particles in *E. coli* inactivation was higher than the hollow counterpart while opposite results were obtained for Qβ phages inactivation and dimethyl sulfoxide (DMSO) degradation. However, their representative of TiO_2 hollow particles was actually opened-hole, cup-liked structure. For the cases which hollow TiO_2 performed better performance, they have explained to be effect of multiple light scattering while described the lower of inactivation

rate of hollow TiO_2 against *E. coli* as contact efficiency decreasing and opened-hole plugging due to larger size of bacteria which prevent the multiple light scattering, thus, decrease PCA (1-2 μm). [14]

CHAPTER III
RESEARCH METHODOLOGY

This research investigates the effects of hollow structure of TiO_2 on photocatalytic antimicrobial activity in comparison with solid counterpart. Dense and hollow TiO_2 particles are synthesized via facile sol-gel approach. Particle size as well as crystalline phase of samples are controlled. For the synthesis of hollow particle, template-assisted method is used to facilitate the formation of TiO_2 shell on the surface of silica nanoparticle template. Silica template is prepared by modified Stöber method, which offers a tunable particle size. To prepare hollow samples, after etching template out with sodium hydroxide solution, acid treatment with hydrochloric acid is applied to eliminate the remaining Na atom on shell surface. This step prevents shell collapsing due to excessive grain growth promoted by Na during calcination. Crystalline phase is controlled with calcination temperature. Anatase can be obtained at calcination temperature lower than 900 °C while rutile requires higher temperature. [15] Dense TiO_2 with the same particle size and crystalline phase as hollow TiO_2 will be prepared in order to conduct the comparative study.

3.1 Chemicals and Materials

1. Tetraethyl orthosilicate (TEOS, 99%)
2. Titanium tetraisopropoxide (TTIP, 99%)
3. Titanium tetrabutoxide (TBT)
4. Methanol (MeOH, 95%)
5. Ethanol (EtOH, 95%)
6. Ammonium hydroxide (NH_4OH, 28% based on NH_3)
7. Sulfuric acid (H_2SO_4, 18 M)
8. Sodium hydroxide (NaOH (s), 99 %)
9. Calcium chloride ($CaCl_2$)
10. Deionized water (DI water)

3.2 Equipment and Apparatus

1. Round-bottom flasks
2. Erlenmeyer flasks
3. Graduated cylinders
4. Volumetric flasks
5. Beakers
6. Watch glass
7. Funnels
8. Crucibles
9. Dropper
10. Pipettes and micropipettes
11. Temperature-controlled magnetic stirrer
12. Magnetic bar
13. Sonicator
14. Centrifuge tubes
15. Centrifuge machine
16. Stands and clamps
17. Spatulas and stirring rod
18. Analytical Balance
19. Oven
20. Muffle furnace
21. Condenser column
22. Petri dish

3.3 Experimental Procedures

3.3.1 Preparation of SiO_2 template

1. Mix desired amount of ammonium hydroxide, deionized water and ethanol in round-bottom flask for 10 minutes.
2. Add silica precursor, TEOS, into previous mixture and stir for 4 hours.
3. Remove unreacted chemicals by centrifuging and re-disperse the resulting particles in ethanol. Repeat washing step three times.

3.3.2 Preparation of hollow TiO_2 nanoparticles [15]

1. Disperse known weight of prepared silica nanoparticle template in EtOH in round-bottom flask.
2. Add deionized water, then stir for 30 minutes.
3. Prepare the mixture of TiO_2 precursor (TBT) in EtOH at volume ratio of 1:4.5 (TBT: EtOH).
4. Raise the temperature of the mixture in step 2 to 85 °C to and stir at 900 rpm under reflux condition. Then slowly add TiO_2 precursor mixture from step 2.
5. Remove unreacted chemicals by centrifugation and re-disperse the resulting particles in EtOH. Repeat washing step three times, then re-disperse the resulting particles in deionized water after the third run of centrifugation to obtain SiO_2/TiO_2 core-shell composites.
6. Add sodium hydroxide solution (2.5 M) into the particles mixture from step 4 and stir for 6 hours. Repeat step 4 but using deionized water instead.
7. Drying in air at 80 °C overnight.
8. Eliminate the leftover Na atom on the surface by mixing particles with 0.5 mmol aqueous sulfuric acid solution (for 150 mg dried solid sample). Stir for 30 minutes.
9. Repeat step 4 but re-disperse in deionized water for the first run and then in EtOH for the rest.
10. Calcine dried samples at the desired temperature and time.

3.3.3 Preparation of dense TiO_2 nanoparticles [16]

1. Prepare 50 ml of MeOH in round-bottom flask.
2. Add $CaCl_2$ solution with the desired concentration as a size regulator and stir for 10 minutes.
3. Gradually add 850 µl TiO_2 precursor (TTIP).
4. Age resulting solution for 24 hours while stirring.
5. Isolate the product by centrifugation, wash with ethanol for two times.
6. Decant the supernatant, dry particles in air at 80 °C.
7. Calcine dried sample at the desired temperature and time.

3.4 Characterization

The synthesized samples will be characterized using TEM, XRD, and UV-DRS. TEM characterization was used to verify morphology and particle size as well as size distribution. After TEM analysis, crystallinity and crystalline phase were examined with XRD. In the last step, optical properties were measured by UV- DRS analysis.

CHAPTER IV
RESULT AND DISCUSSION

In order to compare hollow and dense TiO_2, synthesized nanoparticles were investigated with TEM to check the completion of syntheses. Confirmation can be observed through their morphology and particle size as well as size distribution. Apart from TEM imaging, XRD spectra analysis was employed to distinguish different in crystalline phase between calcined and non-calcined samples. The calcination were actually done at various temperatures (400, 500, 650, and 900 °C), however, the samples became severely aggregated at 500 °C and above. This made further analysis became unavailable. PCA of TiO_2 nanoparticles were evaluated via UV-DRS in term of optical properties. Resulting spectra also reveal the comparison for their optical properties. Finally, bandgap data were calculated from UV-DRS and then used for PCA comparison.

4.1 Morphology of Synthesized Nanoparticles

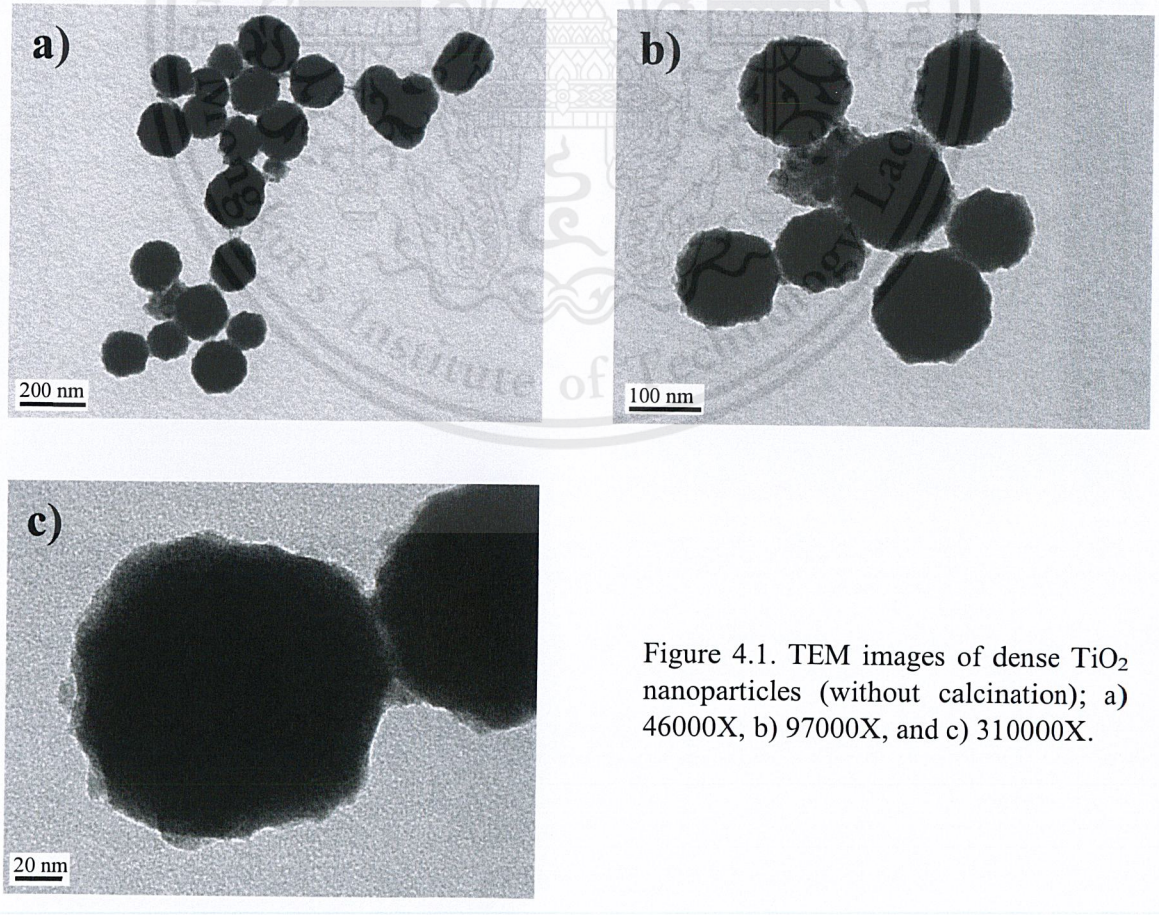

Figure 4.1. TEM images of dense TiO_2 nanoparticles (without calcination); a) 46000X, b) 97000X, and c) 310000X.

Various salt solutions were reported as size regulator agent in dense TiO_2 synthesis. They were described to provide smaller particle size with higher concentration used. [16] In this work, TiO_2 nanoparticles with dense sphere morphology were successfully synthesized using $CaCl_2$ as size regulator agent. Higher concentration of salt solution used result in smaller particle size as demonstrated in the literatures. With 0.0379 M $CaCl_2$ solution employment, the result nanoparticles are shown in Figure 4.1. From TEM image, the particle size is found to be approximately 150 nm.

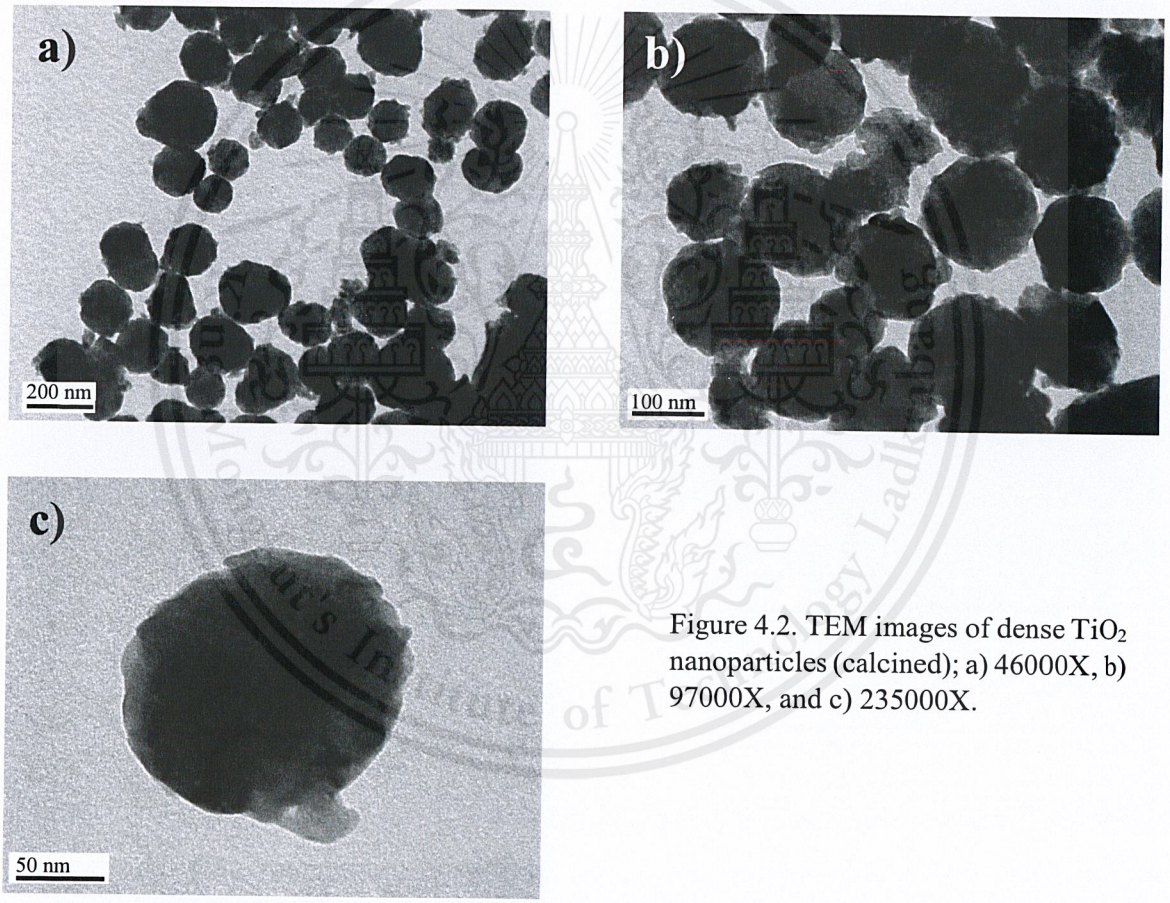

Figure 4.2. TEM images of dense TiO_2 nanoparticles (calcined); a) 46000X, b) 97000X, and c) 235000X.

To obtain anatase phase, TiO_2 nanoparticles were calcined in muffle furnace at different temperature. At temperature beyond 500 °C, the calcined nanoparticles become aggregated severely, thus, cannot be well dispersed as a colloidal mixture. This create a difficulties for further characterization. In order to avoid this issue, lower calcination temperature (400 °C) was used along with longer dwelling time. For the TEM images

shown in this report, 3 hours of calcination at 400 °C was applied. Figure 4.3 and 4.4 show the images of calcined dense and hollow TiO_2 nanoparticles, respectively. Slight shrinkage in size along with more roughness of the surface were observed in the calcined samples.

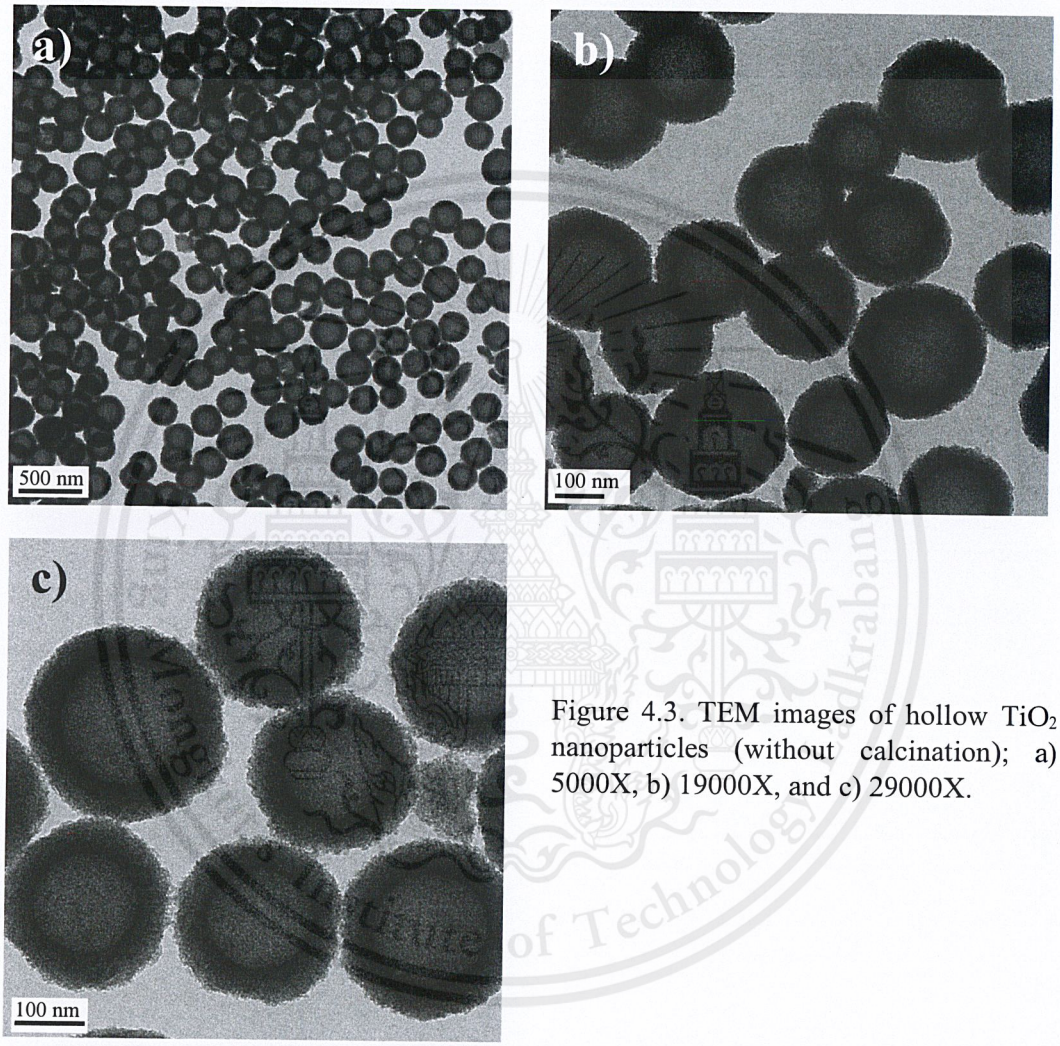

Figure 4.3. TEM images of hollow TiO_2 nanoparticles (without calcination); a) 5000X, b) 19000X, and c) 29000X.

The resulting hollow TiO_2 nanoparticles synthesized by the method purposed by Joo et al. were shown to develop very well-defined hollow morphology along with size distribution. Hollow TiO_2 nanoparticles that were not proceeded through calcination are shown in Figure 4.3. According to TEM images, they are shown to have uniform 50 nm shell thickness and around 125 nm core diameter. For calcined sample, hollow TiO_2 nanoparticles were able to maintain their morphology but the size shrink to approximately 140 nm as revealed by Figure 4.4.

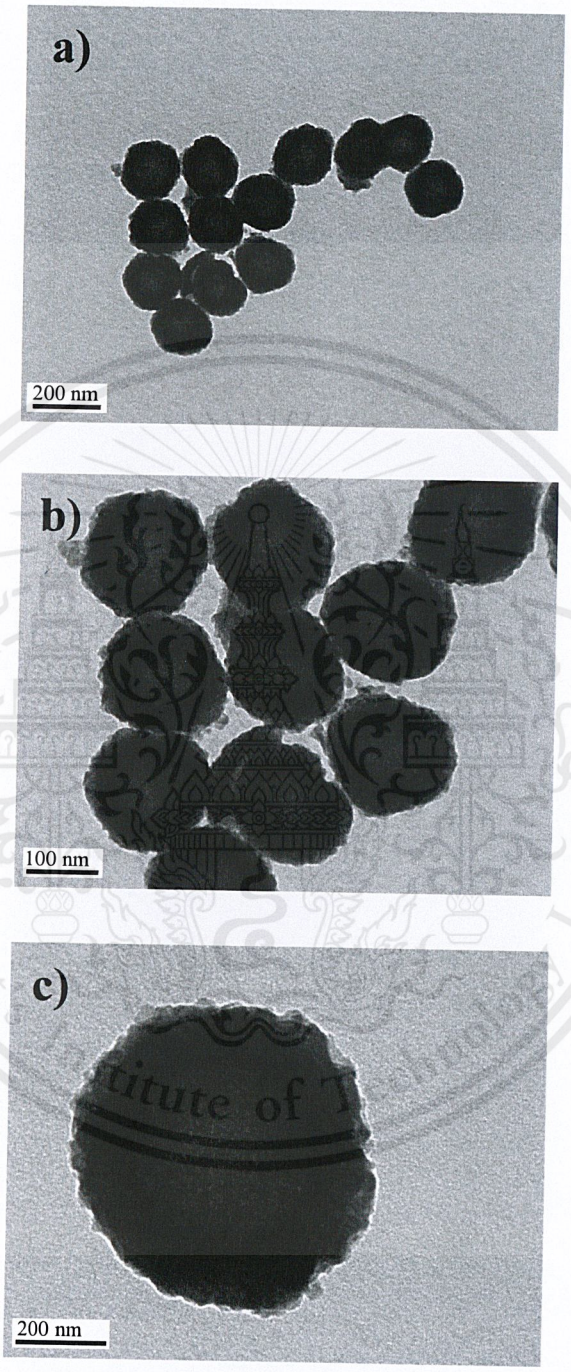

Figure 4.4. TEM images of hollow TiO_2 nanoparticles (calcined); a) 46000X, b) 97000X, and c) 235000X.

4.2 Crystallinity

According to the aggregation issue mentioned above, the calcination was done at 400 °C for 3 hours only. In addition, during XRD test, only calcined and non-calcined hollow TiO2 were used as representatives in crystalline phase characterization for all TiO_2 samples since they are same material with dense TiO_2. According to Figure 4.5, when compared to the reference anatase XRD data, no similar peak were observed. This result indicate that the as-prepared TiO_2 nanoparticles were amorphous. In the same way, this mean that calcined samples were not transformed into anatase yet with current calcining conditions. However, the difference between calcined and amorphous samples were observed with UV-DRS technique, which will be discussed later.

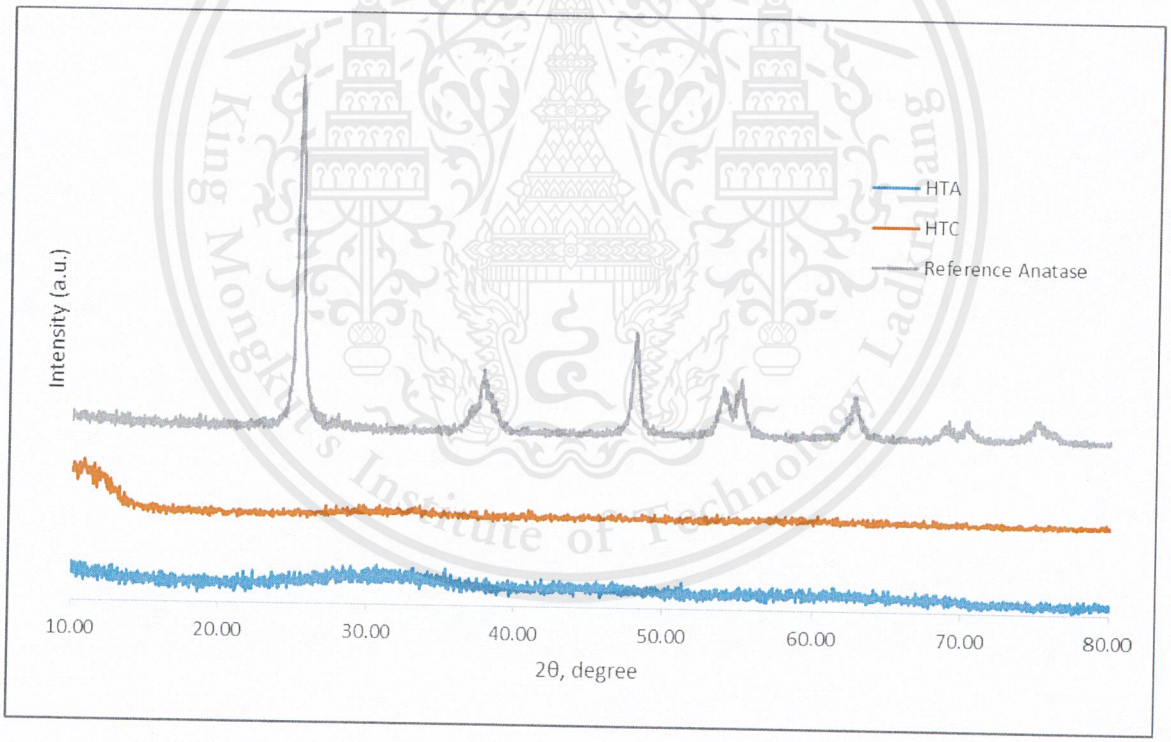

Figure 4.5. XRD Spectra of calcined and non-calcined hollow TiO_2 nanoparticles.

4.3 UV-DRS Spectrum

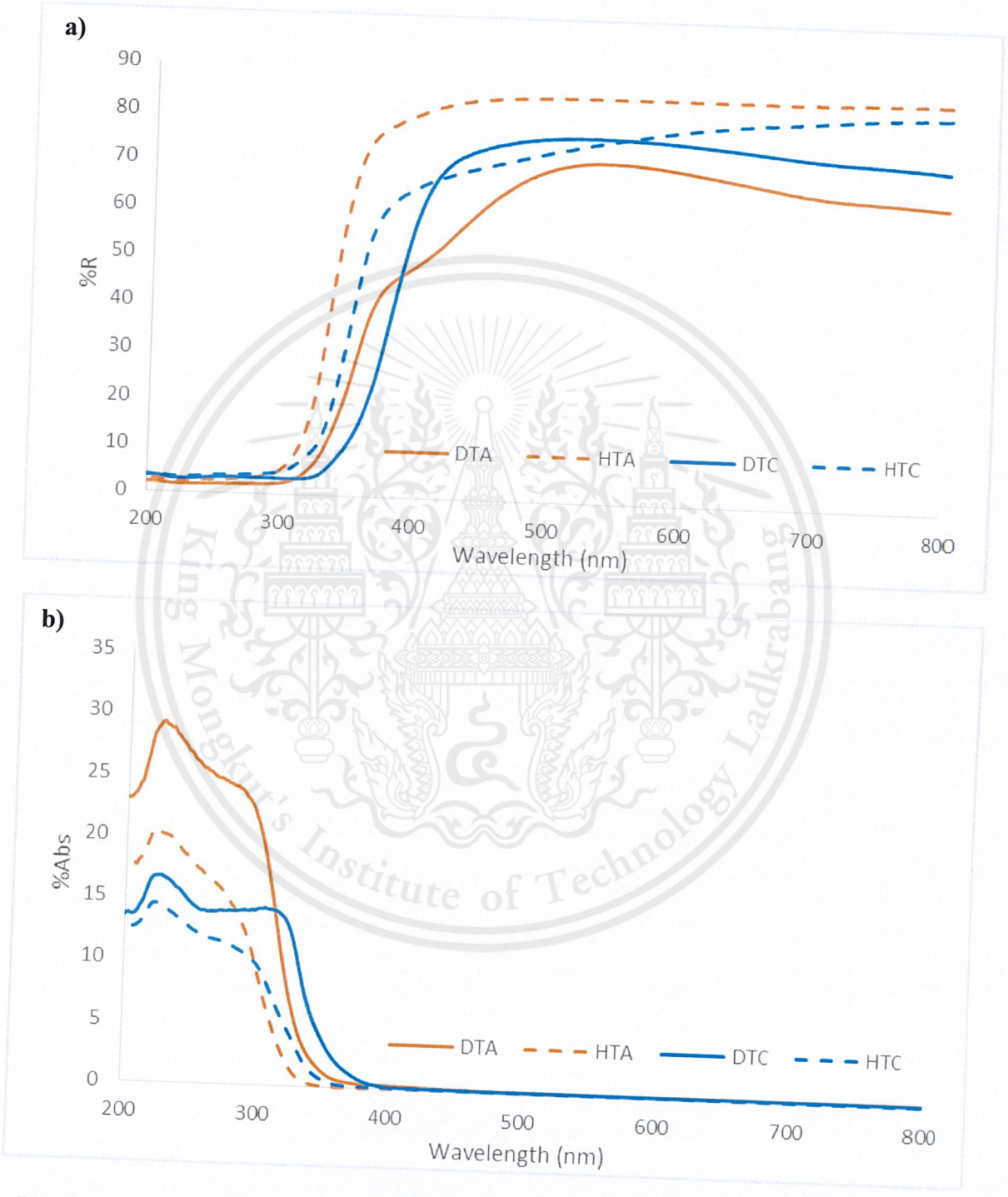

Figure 4.6. UV-DRS Spectrum; a) %Reflectance b) %Absorbance (using Kubelka-Munk function) of amorphous dense TiO_2 (DTA), amorphous hollow TiO_2 (HTA), calcined dense TiO_2 (DTC), and calcined hollow TiO_2 (HTC).

Optical properties were characterized by UV-Vis with integrating sphere attachment, so called UV-DRS. In this characterization, calcined dense and hollow nanoparticles were coded as DTC and HTC, respectively. DTA and HTA were referred to dense and hollow TiO_2 samples without calcination. The resulting spectra are illustrated in Figure 4.6 (a-b). The diffuse reflectance results (%R) in Figure 4.6a were directly measured as raw data with the instrument while the result shown in Figure 4.6b were obtained via transformation of raw data with Kubelka-Munk function into absorbance spectra (%Abs). TiO_2 nanoparticles with hollow morphology were observed to exhibit higher %R and wider range of wavenumber compared to dense TiO_2. Same trend was observed for calcined-samples for morphology comparison. This proves that a hollow cavity can enhance light scattering and reflection which resulted in reflection enhancement.

Since the absence of %R mean absorption is taken place, %Abs is the inverse function of diffuse reflectance. This made the results reported in Figure 4.6a went in opposite trend to which reported in Figure 4.6b. For A% analysis, the first wavenumber of response (cut-off wavelength, λ) is related to the energy that particle can absorbed (bandgap). According to the results, both calcined and non-calcined hollow TiO_2 start to response at higher wavenumber, indicate that they possess higher bandgap energy with respect to dense TiO_2 samples. For comparison in crystalline phase aspect, the calcined samples exhibit lower bandgap energy. Using data from Figure 4.6b, bandgap energy were calculated using equation 4.1 and reported in Table 4.1.

$$Bandgap\ Energy = \frac{h \cdot C}{\lambda} \tag{4.1}$$

Where,

h = Planks constant = 6.626×10^{-34} Joules·sec

C = Speed of light = 3.0×10^{8} meters/sec

λ = Cut-off wavelength

Note that 1 eV = 1.6×10^{-19} Joules (Conversion factor)

Table 4.1. Calculated bandgap energy.

Sample	λ (nm)	Bandgap (eV)
DTA	352	3.53
HTA	333	3.73
DTC	370	3.36
HTC	347	3.58

Considering table 4.1, both hollow TiO_2 samples have higher bandgap energy compared with dense TiO_2. Note that calcined dense TiO_2 sample bandgap energy is very near to those reported generally in anatase TiO_2 (3.2 eV), despite of XRD result which revealed none of anatase characteristic peaks. This means that after calcination, although the crystalline phase was not change, some of polymorph transitioning occurred.

Based on absorbance spectra and calculated band gap energy only, it must be say that in term of PCA, dense TiO_2 samples require less energy to activate the photocatalysis. This made them response to lower energy spectrum of light which provide good trait for the PCA. However, as mention earlier, the concept of multiple light scattering and reflection was proved by the reflectance spectra, consistence with reported by literatures in the field of DSSC application. [12] Moreover, the results reported by Yamaguchi and coworkers also support that PCA can be enhanced through multiple light scattering. These provide a possibility that the actual test which related directly to PCA (e.g. antimicrobial, photodegradation) result may goes against current results. [14] In another word, higher PCA could be observed in hollow TiO_2 samples with such test methods.

In summary, in order to complete the discussion, the test related directly to PCA must be performed to check whether higher diffuse reflectance in hollow TiO_2 can enhance the PCA or not.

CHAPTER V
CONCLUSION

5.1 Conclusion

With the goal to improve TiO_2 photocatalytic acitivity in low light intensity environment, the effect of hollow morphology to the photocatalytic activity was studied. We have synthesized TiO_2 nanoparticles with dense and hollow structures via sol-gel method. Silica template was employed in case of hollow TiO_2 while $CaCl_2$ solution was used for dense TiO_2. TEM images reveal good results for nanoparticles syntheses as they were similar in size, thus, suit for comparison. Calcination at 400 with muffle furnace was applied to prepare anatase samples. Although XRD test provided no peak in all sample, a difference between calcined and non-calcined (amorphous) samples were found in UV-DRS spectrum. The bandgap energy of 3.76 and 3.58 eV were obtained for calcined and non-calcined hollow TiO_2, 3.53 and 3.36 eV for calcined and non-calcined dense TiO_2. For optical properties which relate to PCA, UV-DRS results indicate that hollow TiO_2 samples %R was higher than dense counterparts. This confirms the hypothesis that hollow cavity can enhance the light scattering. On the other hand, considered the bandgap energy of each sample, higher bandgap energy were observed in hollow TiO_2 samples with respect to dense TiO_2 and calcined samples with respect to non-calcined samples.

5.2 Recommendation

With the higher diffuse reflectance in hollow TiO_2 samples and reported data in reviewed literatures, more of characterization that relate directly with PCA like photodegradation and antimicrobial test must be done for the completeness of result discussion. If the final conclusion including the PCA test data reveals that higher diffuse reflectance can really enhance the PCA, in term of improvement based on the current data (bandgap energy), further modification of hollow TiO_2 samples that reduce the bandgap energy could enhance their efficiency along with expand the range of applicability.

REFERENCES

1. Balazs, A. C.; Emrick, T.; Russell, T. P. Nanoparticle Polymer Composites: Where Two Small Worlds Meet. *Science*, 2006, 314(5802), 1107-1110.
2. Cargnello, M.; Gordon, T. R.; Murray, C. B. Solution-phase synthesis of titanium dioxide nanoparticles and nanocrystals. *Chem. Rev.* 2014, 114(19), 9319-9345.
3. Pelaez, M.; Nolan, N. T.; Pillai, S. C.; Seery, M. K.; Falaras, P.; Kontos, A. G.; Dunlop, P. S.M.; Hamilton, J. W.J.; Byrne, J.A.; O'Shea, K.; Entezari, M. H.; Dionysiou, D. D. A review on the visible light active titanium dioxide photocatalysts for environmental applications. *Appl. Catal. B-Environ.* 2012, 125, 331-349.
4. Henderson, M. A. A surface science perspective on TiO_2 photocatalysis. *Surf. Sci. Rep.* 2011, 66(6-7), 185-297.
5. Fujishima, A.; Zhang, X.; Tryk, D. A. TiO_2 photocatalysis and related surface phenomena. *Surf. Sci. Rep.* 2008, 63(12), 515-582.
6. Foster, H. A.; Ditta, I. B.; Varghese, S.; Steele, A. Photocatalytic disinfection using titanium dioxide: spectrum and mechanism of antimicrobial activity. *Appl. Microbiol. Biot.* 2011, 90, 6, 1847-1868.
7. Dahl, M.; Liu, Y.; Yin, Y. Composite titanium dioxide nanomaterials. *Chem. Rev.* 2014, 114(19), 9853-9889.
8. Tian, J.; Zhao, Z.; Kumar, A.; Boughtonc, I. R.; Liu, H. Recent progress in design, synthesis, and applications of one-dimensional TiO_2 nanostructured surface heterostructures: a review. *Chem. Soc. Rev.* 2014, 43(20), 6920-6937.
9. Gao, M.; Zhu, L.; Ong, W. L.; Wanga, J.; Ho, G. W. Structural design of TiO_2-based photocatalyst for H_2 production and degradation applications. *Catal. Sci. Technol.* 2015, 5(10), 4703-4726.
10. Li, G. L., Mohwald, H., & Shchukin, D. G. Precipitation polymerization for fabrication of complex core-shell hybrid particles and hollow structures. *Chem Soc Rev.* 2013, 42(8), 3628-3646.

11. El-Toni, A. M., Habila, M. A., Labis, J. P., Alothman, Z. A., Alhoshan, M., Elzatahry, A. A., & Zhang, F. Design, synthesis and applications of core-shell, hollow core, and nanorattle multifunctional nanostructures. *Nanoscale*. 2016, 8(5), 2510-2531.

12. Dadgostar, S.; Tajabadi, F.; Taghavinia, N. Mesoporous submicrometer TiO_2 hollow spheres as scatterers in dye-sensitized solar cells. *ACS Appl. Mater. Interfaces*. 2012, 4(6), 2964-2968.

13. Zhang, P.; Li, A.; Gong, J. Hollow spherical titanium dioxide nanoparticles for energy and environmental applications. *Particuology*. 2015, 22, 13-23.

14. Yamaguchi, Y.; Shimodo, T.; Usuki, S.; Torigoe, K.; Terashima, C.; Katsumata, K.; Ikekita, M.; Fujishima, A.; Sakaia, H.; Nakata, K. Different hollow and spherical TiO_2 morphologies have distinct activities for the photocatalytic inactivation of chemical and biological agents. *Photochem. Photobiol. Sci.* 2016, 15(8), 988-994.

15. Joo, J. B.; Lee, I.; Dahl, M.; Moon, G. D.; Zaera, F.; Yin, Y. Controllable Synthesis of Mesoporous TiO_2 Hollow Shells: Toward an Efficient Photocatalyst. *Adv. Funct. Mater*. 2013, 23(34), 4246-4254.

16. Han, C., Luque, R., & Dionysiou, D. D. Facile preparation of controllable size monodisperse anatase titania nanoparticles. *Chem. Commun.* 2012, 48(13), 1860-1862.

APPENDIX A:
Experimental Data

Table A.1 Conditions used for hollow TiO_2 nanoparticles synthesis.

Silica template synthesis				
Chemical	TEOS	EtOH	NH_4OH	H_2O
Volume (ml)	0.86	23	0.46	4.3
Temperature	Room temperature			
Reaction time	4 hours			
TiO_2 shell formation				
Chemical	TBT	EtOH	H_2O	
Volume (ml)	4	118	0.48	
Temperature	85 °C, reflux condition			
Reaction time	100 minutes			

Table A.2 Conditions used for dense TiO_2 nanoparticles synthesis.

Dense TiO_2 nanoparticle synthesis			
Chemical	TTIP	MeOH	0.0379M $CaCl_2$ (aq)
Volume (ml)	0.86	50	0.2
Temperature	Room temperature		
Reaction time	24 hours		

Figure A.1 Non-calcined hollow TiO_2 (HTA) XRD result.

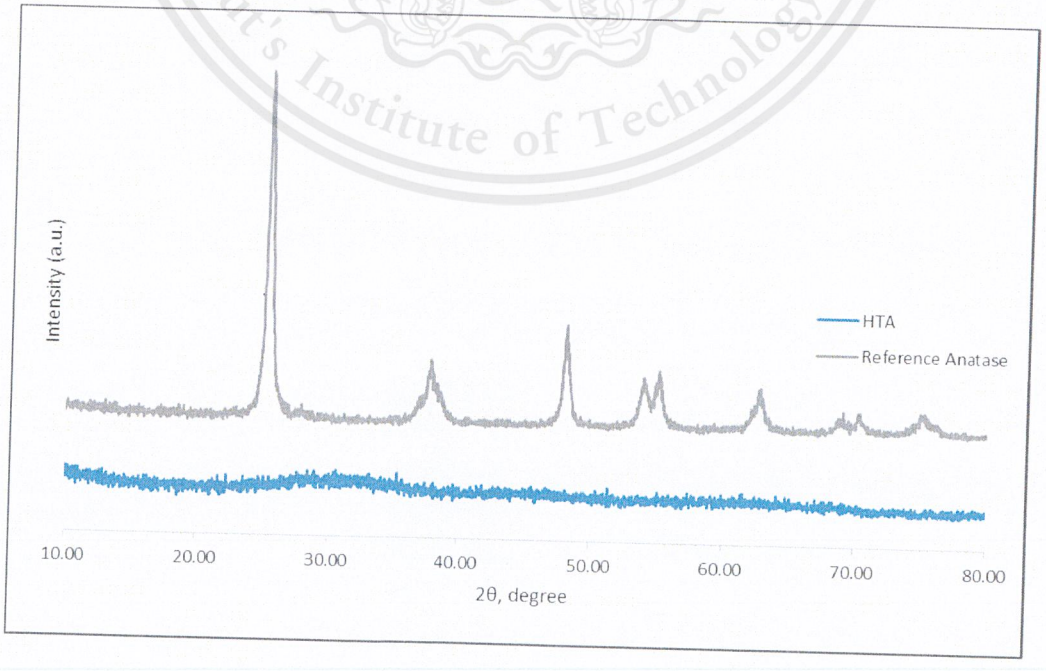

Figure A.2 Calcined hollow TiO_2 (HTC) XRD result.

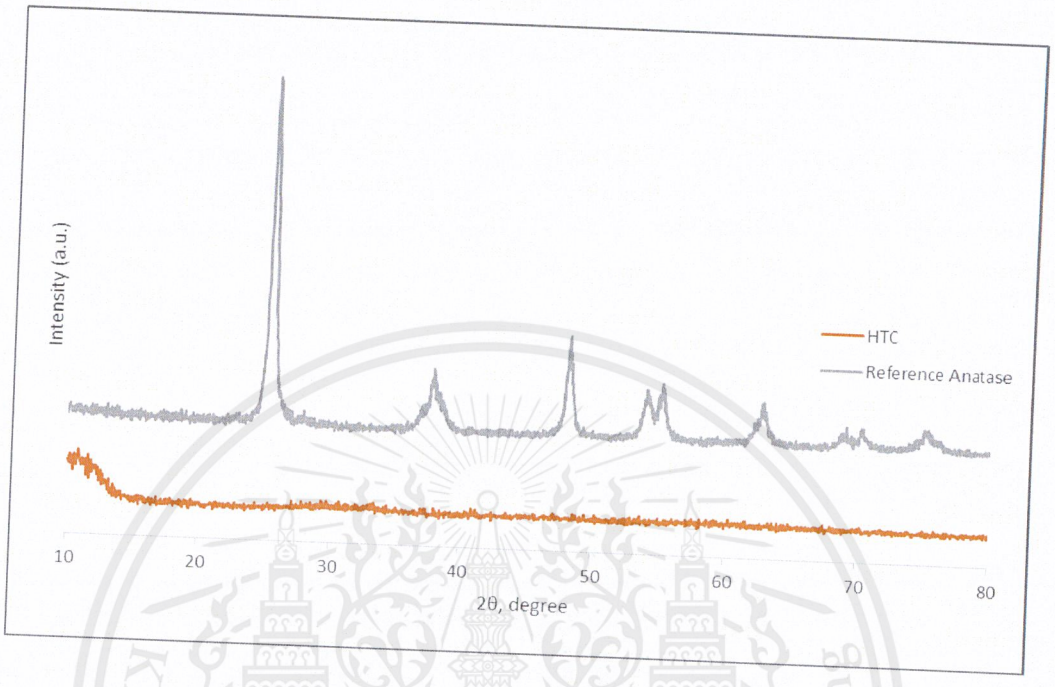

Figure A.3 Non-calcined hollow TiO_2 (HTA) diffuse reflectance spectra.

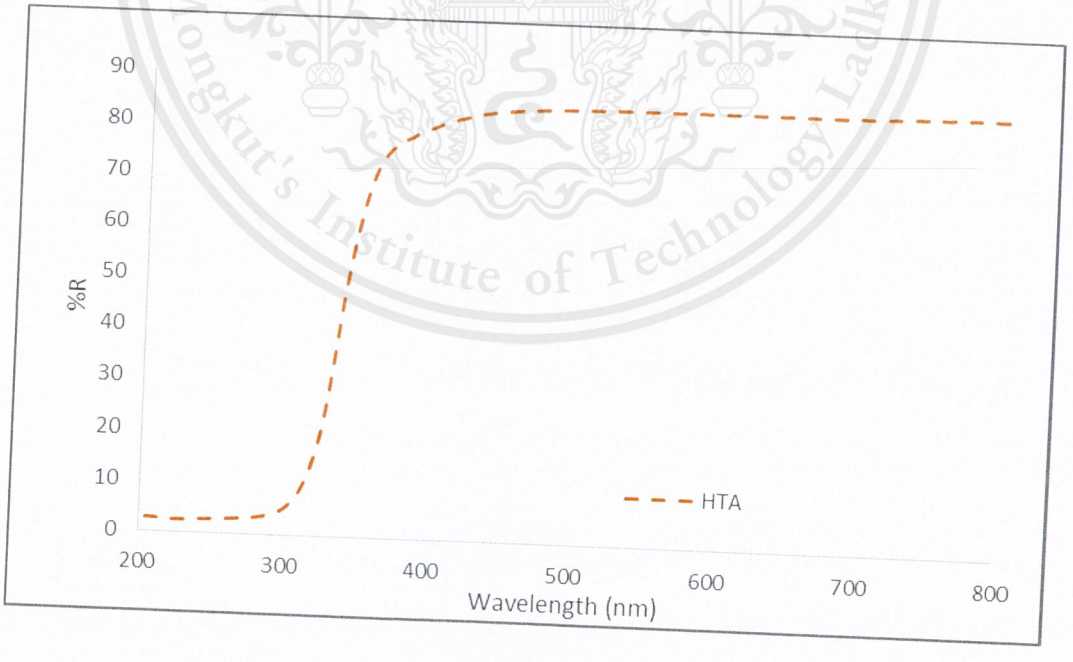

Figure A.4 Calcined hollow TiO_2 (HTC) diffuse reflectance spectra.

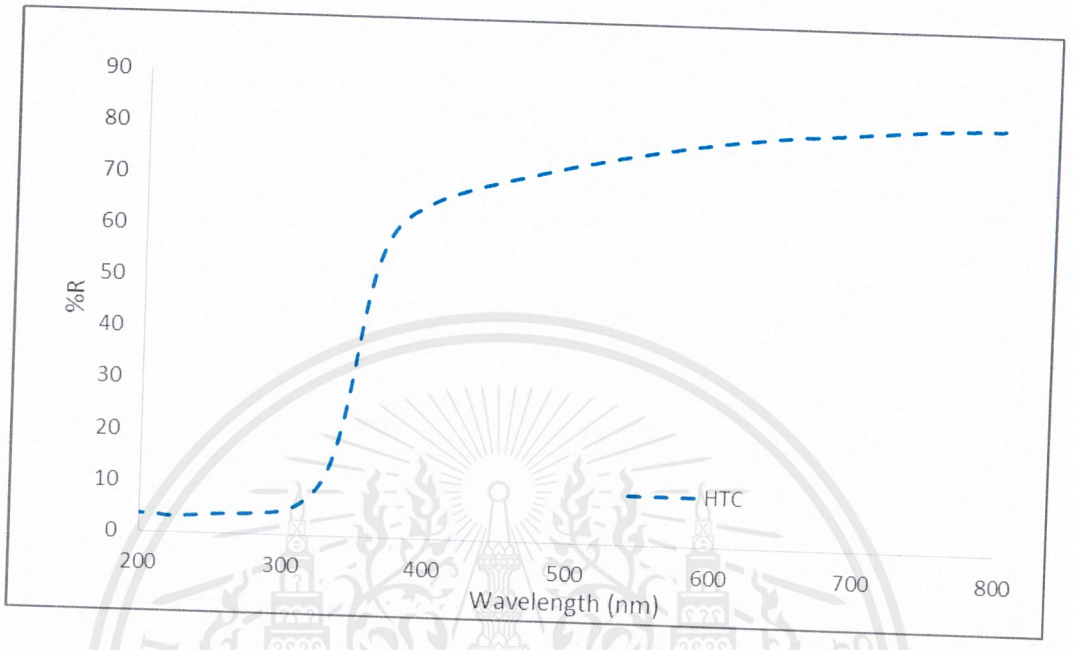

Figure A.5 Non-calcined dense TiO_2 (DTA) diffuse reflectance spectra.

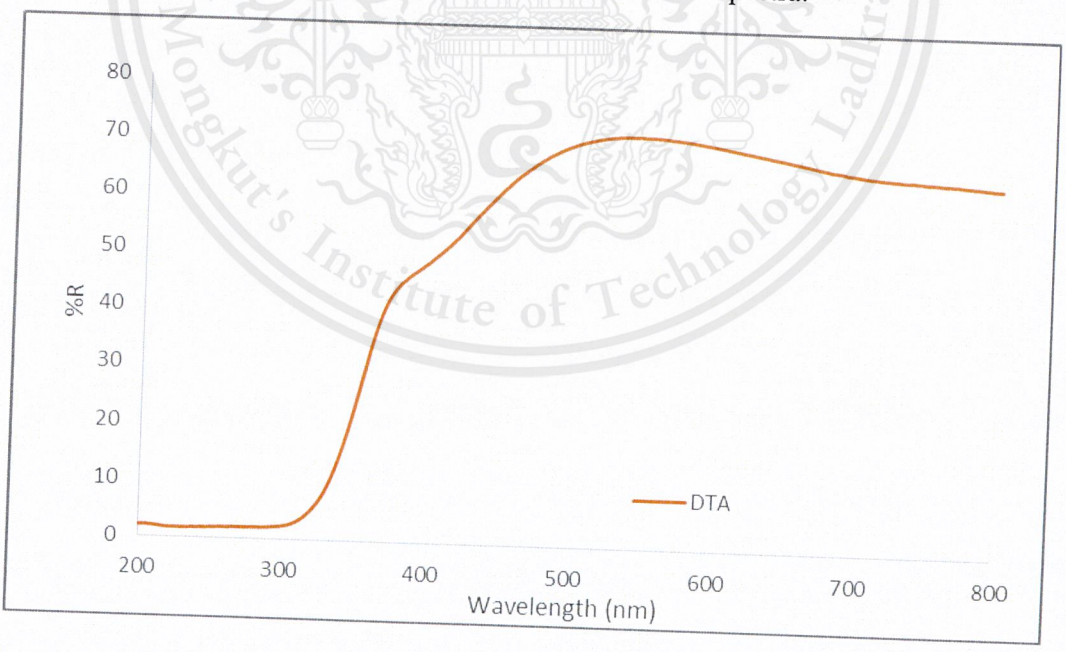

Figure A.6 Calcined dense TiO_2 (DTC) diffuse reflectance spectra.

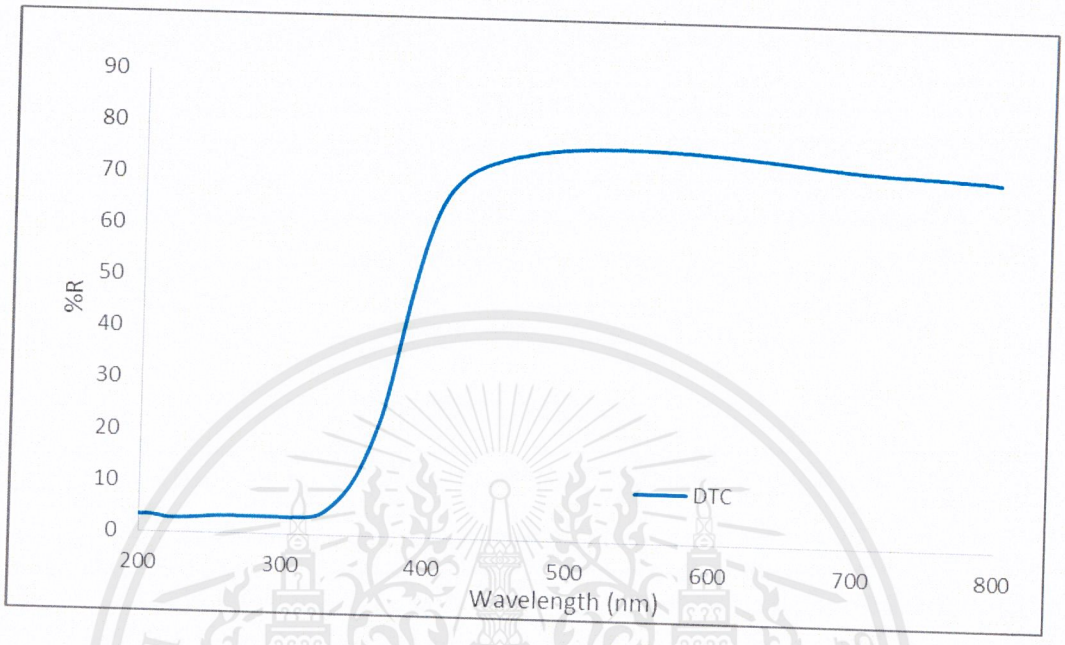

Figure A.7 Non-calcined hollow TiO_2 (HTA) absorbance spectra.

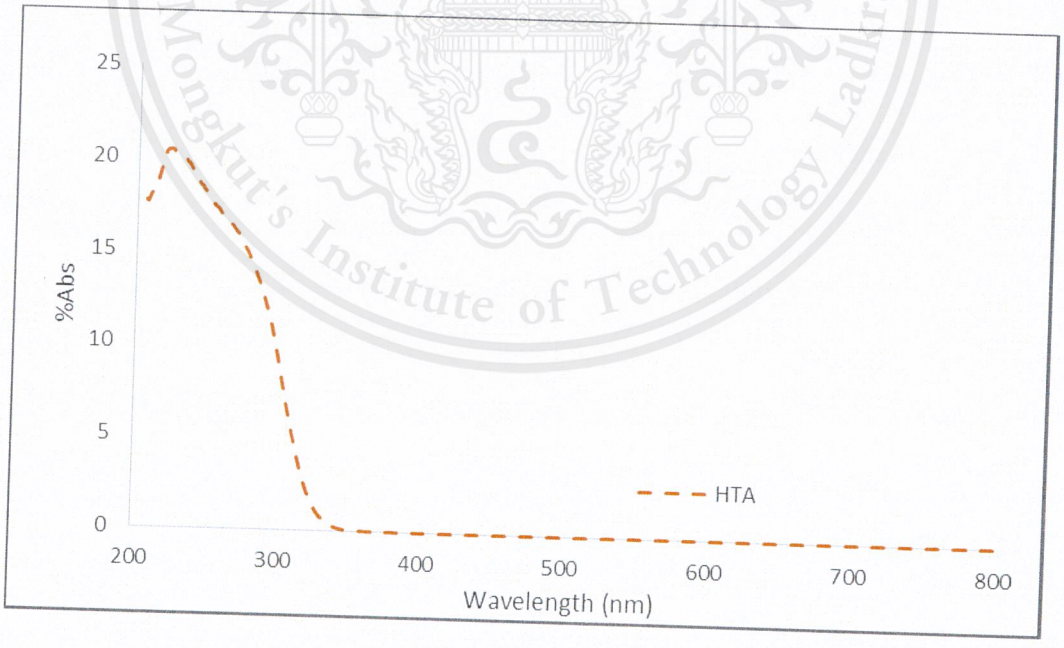

Figure A.8 Calcined hollow TiO_2 (HTC) absorbance spectra.

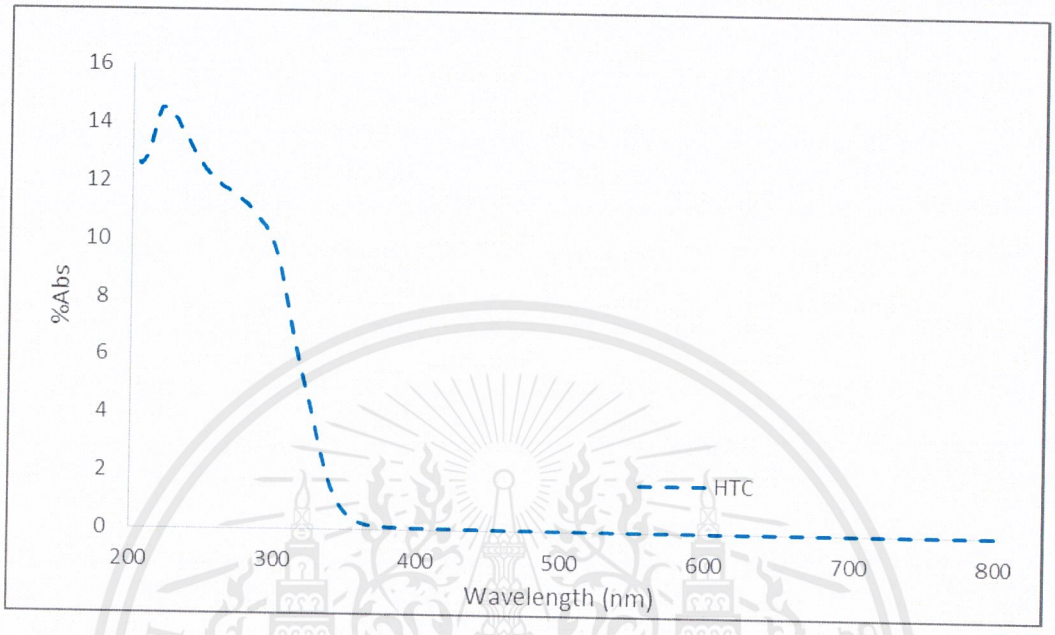

Figure A.9 Non-calcined dense TiO_2 (DTA) absorbance spectra.

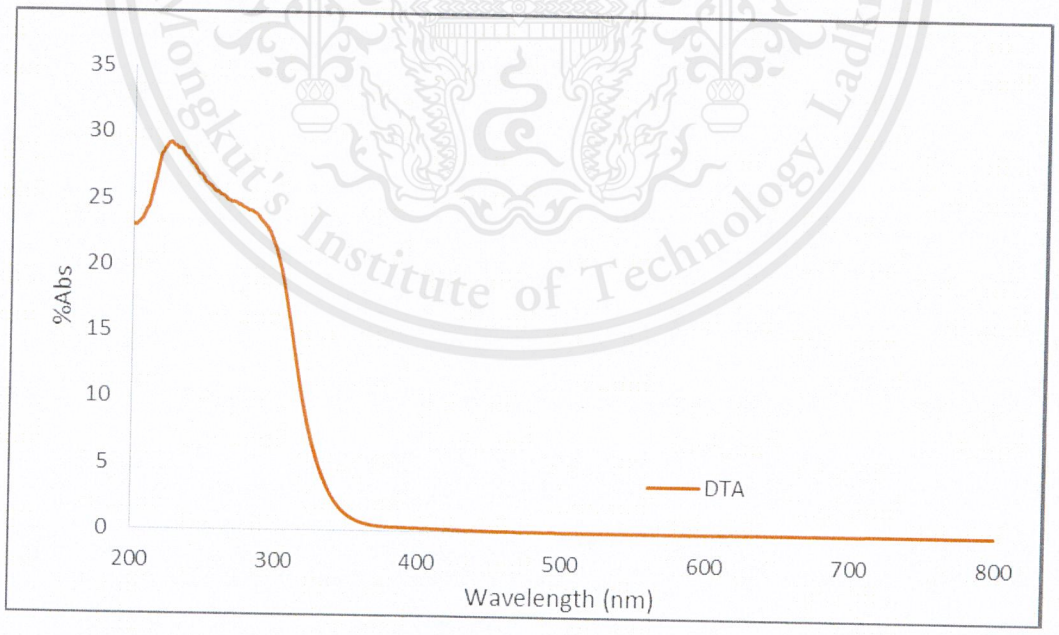

Figure A.10 Calcined dense TiO_2 (DTC) absorbance spectra.

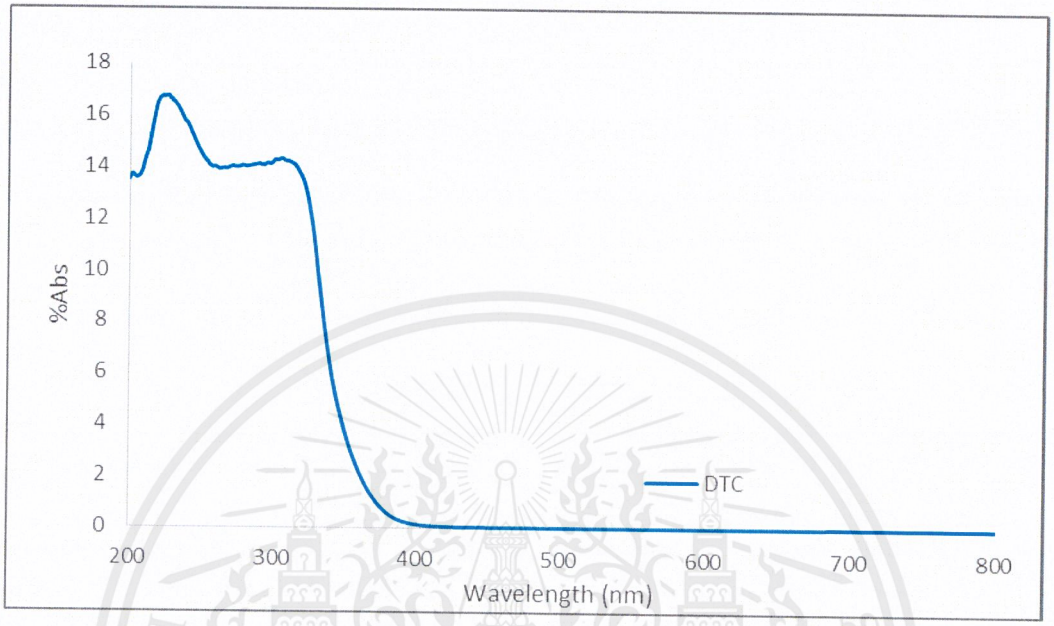

APPENDIX B:

Example of Calculation

Bangdgap Energy Calculation: Non-calcined Hollow TiO2

$$Bandgap\ Energy = \frac{h \cdot C}{\lambda}$$

Where;

h = Planks constant = 6.626 x 10^{-34} Joules·sec

C = Speed of light = 3.0 x 10^{8} meters/sec

λ = HTA Cut-off wavelength = 333 x 10^{-9} meters

Note that 1 eV = 1.6 x 10^{-19} Joules (Conversion factor)

Substitute;

$$Bandgap\ Energy = \frac{(6.626 \times 10^{-34}\ J \cdot s) \cdot (3 \times 10^{8}\ m/s)}{333 \times 10^{-9}\ m}$$

$$Bandgap\ Energy = 5.9694 \times 10^{-19}\ Joules$$

Convert to eV;

$$Bandgap\ Energy = (5.9694 \times 10^{-19}\ Joules) \times \frac{1\ eV}{1.6 \times 10^{-19}\ Joues}$$

$$Bandgap\ Energy = 3.73\ eV$$

BIBLIOGRAHPY

Name: Naphat Thiwakornkitkul

Date of Birth (DD/MM/YY): 08/05/1996

Address: 99/105 Bali Atoll village Kluang-Luangpang Mueng-Chacheongsao Chacheongsao 24000

E-mail: naphat.thiwa@gmail.com

Academic Background: Study in senior year of Petrochemical Engineering Program, Faculty of Engineering, King Mongkut's Institute of Technology Ladkrabang.

Working Experience: -